Cancer Letters 457 (2019) 180–190

Contents lists available at ScienceDirect

Cancer Letters

journal homepage: www.elsevier.com/locate/canlet

Original Articles

Hepatoma-derived growth factor supports the antiapoptosis and profibrosis of pancreatic stellate cells

Yi-Ting Chen[a,b,1], Feng-Wei Chen[c,1], Tsung-Hao Chang[c], Tso-Wen Wang[a], Teng-Po Hsu[d], Jhih-Ying Chi[a], Yu-Wei Hsiao[a], Chien-Feng Li[b,e,*], Ju-Ming Wang[a,f,g,h,**]

[a] Department of Biotechnology and Bioindustry Sciences, College of Bioscience and Biotechnology, National Cheng Kung University, Tainan, Taiwan
[b] Medical Research Department, Chi Mei Medical Center, Tainan, Taiwan
[c] Institute of Basic Medical Science, College of Medicine, National Cheng Kung University, Tainan, Taiwan
[d] Department of Life Sciences, College of Bioscience and Biotechnology, National Cheng Kung University, Tainan, Taiwan
[e] Department of Pathology, Chi Mei Medical Center, Tainan, Taiwan
[f] International Research Center for Wound Repair and Regeneration, National Cheng Kung University, Tainan, Taiwan
[g] Graduate Institute of Medical Sciences, College of Medicine, Taipei Medical University, Taipei, Taiwan
[h] Graduate Institute of Medicine, College of Medicine, Kaohsiung Medical University, Kaohsiung, Taiwan

ARTICLE INFO

Keywords:
Hepatoma-derived growth factor (HDGF)
Pancreatic stellate cells (PSCs)
Antiapoptosis
And profibrosis

ABSTRACT

Pancreatic cancer is refractory and is characterized by extensively surrounding and intratumor fibrotic reactions that are contributed by activated pancreatic stellate cells (PSCs). Herein, we show that CCAAT/enhancer-binding protein δ (CEBPD) responds to transforming growth factor-β1 (TGF-β1) through reciprocal loop regulation and that activated hypoxia inducible factor-1α (HIF-1α) further contributes to the upregulation of the hepatoma-derived growth factor *(HDGF)* gene. Secreted HDGF contributes to the antiapoptosis of PSCs and consequently leads to the synthesis and deposition of extracellular matrix proteins for stabilizing PSC/pancreatic cancer cell (PCC) tumor foci. This result agrees with the observation that severe stromal growth positively correlated with stromal HDGF and CEBPD expression in pancreatic cancer specimens. Collectively, the identification of the TGF-β1-activated CEBPD/HIF-1α/HDGF axis provides new insights into novel discoveries of HDGF in the antiapoptosis and profibrosis of PSCs and the outgrowth of PCCs.

1. Introduction

A strong fibrotic reaction leads to a fibrotic hypovascular barrier that surrounds pancreatic tumors, resulting in poor blood perfusion in transplanted tumors, in contrast to a normal pancreas [1]. Pancreatic stellate cells (PSCs) are a subset of pancreatic cancer-associated fibroblasts that regulate the synthesis and degradation of *extracellular matrix* (ECM) proteins and provide prosurvival signals to tumors [2–4]. In response to TGF-β1, PSC activation enhances proliferative rates and differentiated transformation into myofibroblast-like cells and increases the secretion of ECM proteins, particularly collagens [3]. In addition, although the hypoxia-induced profibrotic and proangiogenic responses in PSCs have been established in pancreatic cancer progression [5,6], the interaction between PSCs and PCCs in the early stage with normoxia remains largely uninvestigated.

However, recent studies used an α-smooth muscle actin (α-SMA)-positive myofibroblast-depleted model [7] or a sonic hedgehog-deficient mouse model [8] and reported a surprising role of fibrosis in pancreatic cancer to restrain tumor growth through depletion or reduction of stromal fibrotic content. These findings suggest that the PSC-generating fibrotic microenvironment is important not only for passive scaffold architecture but also as an active regulator of tumors. Hence, targeting the interaction between tumor and stromal tissues has been suggested as a potential strategy for pancreatic tumor treatment [9].

Following tumorigenesis, the cancer cell-faced environment initiates from normoxic conditions. Hypoxia inducible factor-1α (HIF-1α) is an inducible transcription factor that is generally stable under hypoxic conditions [10]. In tumorigenesis, the inactivation of transcription factor CCAAT/enhancer-binding protein δ (CEBPD) in certain cancer cells has been suggested to benefit cancer progression [11,12].

* Corresponding author. Department of Pathology, Chi Mei Medical Center, Tainan, Taiwan.
** Corresponding author. Department of Biotechnology and Bioindustry Sciences, College of Bioscience and Biotechnology, National Cheng Kung University, Tainan, Taiwan.
E-mail addresses: cfli@mail.chimei.org.tw, angelo.p@yahoo.com.tw (C.-F. Li), yumingw@mail.ncku.edu.tw, wwwjm4721@yahoo.com.tw (J.-M. Wang).
[1] Yi-Ting Chen and Feng-Wei Chen are equally contributed to this manuscript.

https://doi.org/10.1016/j.canlet.2019.05.001
Received 10 December 2018; Received in revised form 30 March 2019; Accepted 2 May 2019

Activation of CEBPD in the tumor microenvironment has been suggested to serve a protumor role [13,14]. Hypoxia induces CEBPD induction [15], and CEBPD directly binds to the HIF-1α promoter to regulate HIF-1α expression and transcriptional activity [16]. Although the involvement and importance of HIF-1α in cancer progression in hypoxia has been fully supported, the regulation and participation of HIF-1α and CEBPD in stromal fibroblasts, particularly in stellate cells, under normoxic conditions remain uninvestigated.

Hepatoma-derived growth factor (HDGF) has been suggested to play a protumor role in the promotion of hepatoma cell proliferation [17,18], metastasis [19], invasion, epithelial-mesenchymal transition [20], and angiogenesis [21]. The divergent HDGF functions participate in a broad range of cancer cell activities. Moreover, HDGF protein is detectable and increased in the secretome of activated PSCs compared to quiescent PSCs [22]. However, to our knowledge, the involvement and effect of HDGF on pancreatic cancer-associated fibrosis, including its role in PSCs and its associated contribution in cancer progression, remains an open question.

In the current study, we demonstrated that HDGF was secreted from TGF-β1-treated PSCs and contributed to antiapoptosis and the generation of an ECM protein-rich microenvironment. We further revealed that the consequent activation of CEBPD and HIF-1α was involved in the transcriptional activation of *HDGF* gene in PSCs. Stromal HDGF and CEBPD are positively associated with the severe stromal growth of pancreatic cancers. In addition to providing new insights into HDGF and CEBPD biology in pancreatic cancer, these results also suggest that HDGF and CEBPD could serve as fibrotic markers for developing an inhibitor of fibrotic reactions.

2. Materials and methods

2.1. Cell culture

Immortalized human pancreatic stellate cells (RTL-PSCs) were generously provided by Dr. Kelvin K.C. Tsai (National Health Research Institutes, Taiwan [23]). RTL-PSCs were maintained in DMEM. Human pancreatic cancer cell lines, PANC-1 and MIA PaCa-2, were generously provided by Dr. Yan-Shen Shan (National Cheng Kung University Hospital, Taiwan [24]). PANC-1 and MIA PaCa-2 cells were maintained in RPMI-1640 medium. Details of cell culture are available in the Supplementary Information.

2.2. Recombinant human TGF-β1, HDGF and chemical inhibitor reagents

Detailed information is provided in the Supplementary Information.

2.3. Reverse transcription polymerase chain reaction (RT-PCR), quantitative PCR (qPCR), and Western blot assays

Details are available in the Supplementary Information. The specific primer sequences of target gene amplification and reaction conditions are listed in Supplementary Tables 1 and 2; the conditions of primary and secondary antibodies in the Western blot assay are listed in Supplementary Table 3.

2.4. Propidium iodide (PI) staining and caspase-3/7 activity for apoptosis analysis

Methyl methanesulfonate (MMS; Sigma-Aldrich Co., St. Louis, Missouri, United States; #129925) was used to induce cell death through apoptosis. Treated cells were subjected to PI staining or caspase-3/7 activity determination. Details are provided in the Supplementary Information.

2.5. Lentiviral short hairpin RNA (shRNA) system

Expression vectors (pLKO AS3w.puro and pLKO AS3w.eGFP.puro) and other target genes of shRNAs were purchased from the National RNAi Core Facility Platform of Academia Sinica in Taiwan. Details are available in the Supplementary Information.

2.6. Hanging drop cell culture for a three-dimensional coculture system of PSCs and PCCs

PCCs expressing enhanced green fluorescence protein (EGFP/PANC-1 or EGFP/MIA PaCa-2 cells) were individually mixed with mCherry-bearing RLT-PSCs (mCherry/*shLacZ* RLT-PSCs or mCherry/*shHDGF* RLT-PSCs). Several drops of mixed cells containing Matrigel matrix were seeded onto a glass bottom using hanging drop cell culture. Details are available in the Supplementary Information.

2.7. Animal xenograft model for the coimplantation of RLT-PSCs and PCCs

shLacZ or *shHDGF* RLT-PSCs were individually mixed with EGFP/PANC-1 or EGFP/MIA PaCa-2 cells. The mixed cells were subcutaneously injected into the right flank of nonobese diabetic/severe combined immunodeficient mice. After nine weeks, subcutaneous tumors were evaluated using an *in vivo* imaging system and dissected and applied for the following experiments. Details are available in the Supplementary Information.

2.8. Immunofluorescence (IF) analysis

Cells, 4 μm of paraffin-embedded mouse sections, and a commercial tissue array with 78 human primary pancreatic adenocarcinoma specimens (purchased from US Biomax, Inc., Derwood, Maryland, United States; # PA961b) were used for IF analysis. Detailed procedures are available in the Supplementary Information.

2.9. Picrosirius red staining, immunohistochemistry (IHC) analysis, TdT-mediated dUTP nick end labeling (TUNEL) assay, enzyme-linked immunosorbent assay (ELISA), transcription factor prediction, and chromatin immunoprecipitation (ChIP) assay

Detailed procedures are available in the **Supplementary Information**.

2.10. Plasmid transfection, reporter plasmid construction and luciferase reporter assay

A human HIF-1α expressing vector (pCEP4/HIF-1α) and two promoter fragments of the human *HDGF* gene cloned into pGL3-Enhancer vectors (pHDGF 2047: −2017 to +30 and pHDGF 876: −774 to +102) were kindly provided by Professor Shaw-Jenq Tsai (National Cheng Kung University; Taiwan) and Professor Ming-Hong Tai (National Sun Yat-sen University, Taiwan), respectively. The pcDNA3/HA-CEBPD expressing vector was established as previously described [25]. Other details are available in the Supplementary Information.

2.11. Statistical analysis

GraphPad Prism 5 software (GraphPad Software, Inc., La Jolla, California, United States) was used to assess statistical significance. Statistical significance was assessed in cell-based *in vitro* assays, animal studies, and clinical specimens using Student's *t*-test, the Mann-Whitney *U* test, or Pearson's correlation coefficient test.

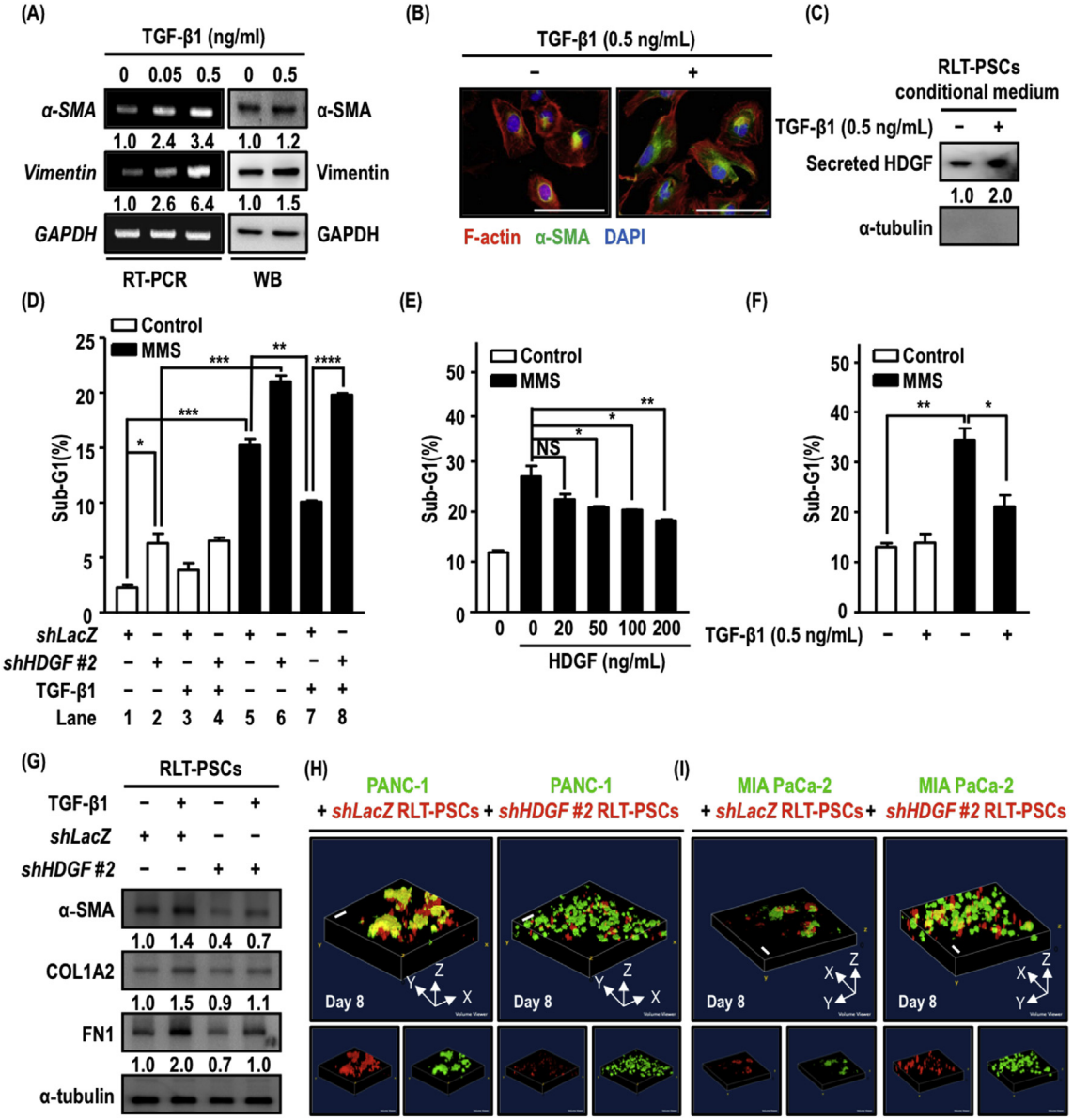

Fig. 1. Hepatoma-derived growth factor (HDGF) exerts antiapoptotic and profibrotic effects on pancreatic stellate cells (PSCs) that interact with pancreatic cancer cells (PCCs).(A) RLT-PSCs (immortal human PSCs) were treated with transforming growth factor-β1 (TGF-β1) in a dose-dependent manner for 24 h. The fibrogenic markers in TGF-β1-treated RLT-PSCs, α-smooth muscle actin (α-SMA) and vimentin, were further determined using reverse transcription-polymerase chain reaction (RT-PCR) and Western blot (WB) assays. (B) Immunofluorescence staining was used to examine the fibrogenic markers in TGF-β1-treated RLT-PSCs, such as the high expression of α-smooth muscle actin (α-SMA) and filamentous actin (F-actin) rearrangement. α-SMA expression and F-actin rearrangement were determined in RLT-PSCs treated with or without TGF-β1 (0.5 ng/mL) for 24 h. Immunofluorescence staining images were captured under a vertical fluorescence microscope to observe morphological changes (white scale bar, 100 μm). Green and red fluorescence indicate the expression of α-SMA and F-actin, respectively. (C) The conditioned medium was collected and concentrated from RLT-PSCs with or without TGF-β1 treatment (0.5 ng/mL) for 24 h. Secreted HDGF expression was determined using Western blot assays, and α-tubulin served as a negative control to exclude signals from the cell lysate of RLT-PSCs. (D) to (F) Methyl methanesulfonate (MMS) treatment was used to induce cell death. Treated RLT-PSCs were harvested and subjected to an analysis of the cell cycle distribution by flow cytometry using propidium iodide staining. The sub-G1 phase indicated the apoptotic cell population. shLacZ (control) or shHDGF #2 (HDGF knockdown) RLT-PSCs were established by lentivirus-delivered short hairpin RNAs. shLacZ, shHDGF #2 (D) or parental (E and F) RLT-PSCs were pretreated with recombinant human HDGF as indicated (0, 20, 50, 100, and 200 ng/mL) for 6 h or TGF-β1 (0.5 ng/mL) for 24 h. MMS (75 μg/mL) was administered to pretreated cells for 24 h. (G) Expression of α-SMA, type I collagen (COL1A2), and fibronectin (FN1) was determined in shLacZ and shHDGF #2 RLT-PSCs under TGF-β1 stimulation (0.5 ng/mL) for 24 h by Western blot assays. (H) and (I) shLacZ or shHDGF #2 RLT-PSCs were transfected with the mCherry fluorescent gene (mCherry/shLacZ RLT-PSCs or mCherry/shHDGF #2 RLT-PSCs, respectively). PCCs, PANC-1 and MIA PaCa-2 cells were transfected with the enhanced green fluorescent protein (EGFP) gene (EGFP/PANC-1 or EGFP/MIA PaCa-2 cells). The mCherry/shLacZ RLT-PSCs or mCherry/shHDGF #2 RLT-PSCs were individually cocultured with EGFP/PANC-1 or EGFP/MIA PaCa-2 cells. The mixed mCherry/RLT-PSCs and EGFP/PCCs (ratio = 5:1) were suspended in 50% Matrigel and subjected to a three-dimensional system by hanging drop cell culture. After 8 days, the sphere structure was observed at 100 × magnification and captured by confocal microscopy (white scale bar, 200 μm). According to the z-section of the captured images, the fluorescence intensity was remodeled to reconstruct the three-dimensional structure by ImageJ software. The above data are presented as the mean ± standard error of the mean from three independent experiments, and the statistical significance was determined using Student's unpaired *t*-test (*P < 0.05; **P < 0.01; ***P < 0.001; ****P < 0.0001). (For interpretation of the references to color in this figure legend, the reader is referred to the Web version of this article.)

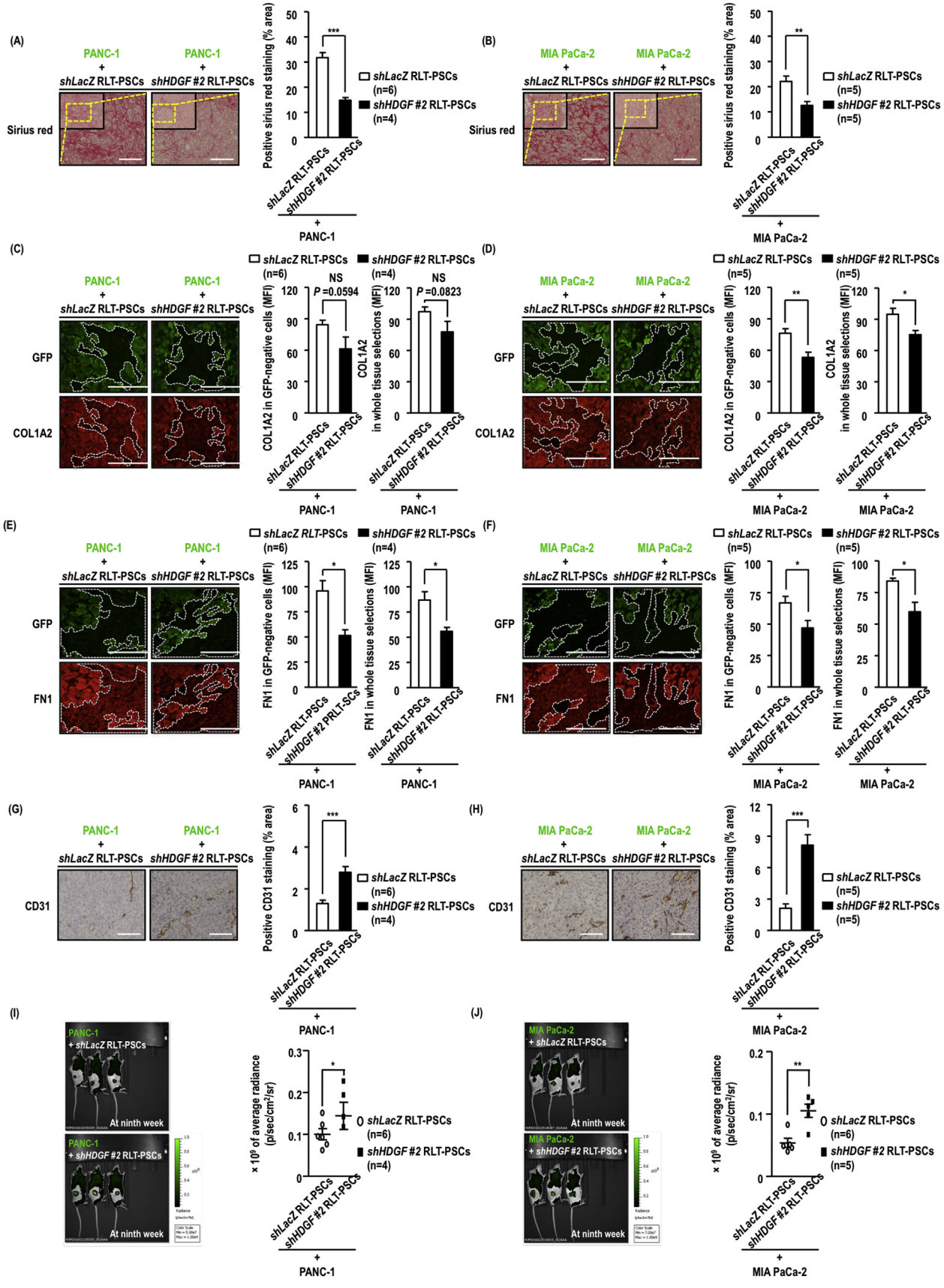

(caption on next page)

Fig. 2. HDGF-knockdown PSCs attenuate fibrotic effects and influence the outgrowth of PCCs *in vivo*.shLacZ RLT-PSCs or shHDGF #2 RLT-PSCs were individually mixed with EGFP/PCCs (EGFP/PANC-1 or EGFP/MIA PaCa-2 cells). The mixture of RLT-PSCs and EGFP/PCCs (ratio = 1:1) containing 50% Matrigel was subcutaneously injected into nonobese diabetic-severe combined immunodeficient mice. Each group contained 4 to 6 mice. After mice were sacrificed at the ninth week, tissue sections of subcutaneous tumors were subjected to immunofluorescence, Picrosirius red staining, and immunohistochemistry analysis. (A) and (B) Picrosirius red staining was applied to evaluate the expression of collagens. The images (left upper panels) were observed at 100 × magnification; the areas bound by the yellow dotted line were observed at 200 × magnification under a vertical microscope, and the captured images are shown as the right lower panels (white scale bar, 100 μm). Red color indicates positive staining of collagens, which were quantified in the right panels. (C) to (F) Expression of COL1A2, FN1, and green fluorescent protein (GFP) was determined using immunofluorescence staining. The images were observed at 400 × magnification under a vertical microscope (white scale bar, 100 μm). GFP expression in the upper panels indicates the locations of PCCs. The white dashed line circles the regions of GFP-negative cells representing stromal cells. The mean fluorescence intensity (MFI) of COL1A2 and FN1 in GFP-negative cells was quantified by ImageJ software and is shown in the right panels. (G) and (H) Immunohistochemistry assays were performed to determine the tumor vasculature by staining with the endothelial cell marker CD31. The images were observed at 200 × magnification (white scale bar, 100 μm); the brown color indicates positive staining of CD31 expression, which was quantified in the right panels. (I) and (J) IVIS spectrum was applied to evaluate tumor growth in the coimplantations of RLT-PSCs and PCCs according to the intensity of green fluorescence expressed in EGFP/PANC-1 or EGFP/MIA PaCa-2 cells. The above results are presented as the mean ± standard error of the mean; the statistical significance was determined using Student's unpaired *t*-test (NS stands for not significant; *P < 0.05; **P < 0.01; ***P < 0.001; ***P < 0.0001). (For interpretation of the references to color in this figure legend, the reader is referred to the Web version of this article.)

3. Results

3.1. HDGF is responsive to TGF-β1 in PSCs and plays antiapoptotic and profibrotic roles in pancreatic cancer

TGF-β1, which mediates fibrosis, is upregulated and secreted in pancreatic tumors [26,27]. *α-SMA* transcripts are responsive to TGF-β1 in RLT-PSCs (immortal human PSCs) [28]. We verified fibrogenic markers in TGF-β1-treated RLT-PSCs. The results showed that TGF-β1 induced the expression of α-SMA and vimentin (Fig. 1A). Moreover, the RLT-PSCs showed a morphological change into a myofibroblast-like shape that exhibited F-actin rearrangements and higher migration activity (Fig. 1B **and** Supplementary Fig. 1). We next verified whether HDGF expression is responsive to TGF-β1 in PSCs. The results showed that the secretion of HDGF is increased in the conditioned medium of TGF-β1-treated RLT-PSCs (Fig. 1C).

Physically, an increased cell number results from cell proliferation and survival. Although the involvement of HDGF in the proliferation of fibroblasts was previously suggested [29], we further found that the attenuation of HDGF could induce the apoptosis of RLT-PSCs (Fig. 1D**, lanes 1 and 2;** Supplementary Fig. 2B). Moreover, we found that HDGF-treated RLT-PSCs were resistant to apoptotic activator methyl methanesulfonate (MMS)-induced cell apoptosis (Fig. 1E). Following the confirmation that TGF-β1 could suppress the MMS-induced apoptosis of RLT-PSCs (Fig. 1F), we found that the antiapoptotic effect was attenuated in *shHDGF* RLT-PSCs (Fig. 1D**, lanes 5 to 8;** Supplementary Fig. 2B). These results suggest that HDGF is required for the TGF-β1-induced antiapoptotic effect in MMS-treated RLT-PSCs. Additionally, the inhibition of HDGF also attenuated the expression of TGF-β1-induced fibrogenic markers, including α-SMA, type I collagen (COL1A2) and fibronectin (FN1) (Fig. 1G**;** Supplementary Fig. 2C). These results suggest that HDGF, at least in part, contributes to antiapoptosis and ECM protein synthesis in PSCs.

PSCs have been suggested to accompany and closely interact with PCCs [30]. To address the effect of HDGF on the cell-cell interaction of PSCs and PCCs, RLT-PSCs and PCCs were cocultured using a hanging drop cell culture system. mCherry-bearing *shLacZ* RLT-PSCs or *shHDGF* RLT-PSCs (mCherry/*shLacZ* RLT-PSCs or mCherry/*shHDGF* RLT-PSCs; Supplementary Fig. 2D) were individually cocultured with EGFP-bearing PCCs (EGFP/PANC-1 or EGFP/MIA PaCa-2 cells; Supplementary Fig. 2E). Regarding the z-sections of the captured images, compared with mCherry/*shLacZ* RLT-PSCs, the constituted images showed that the colocalizing signals of the composite spheres were diminished when EGFP/PANC-1 or EGFP/MIA PaCa-2 cells were cocultivated with mCherry/*shHDGF* RLT-PSCs (Fig. 1H and I**;** Supplementary Figs. 2F and 2G**;** Supplementary Movies 1 and 2). These results suggest that stromal HDGF contributes to cell-cell interaction of PSCs and PCCs and is able to stabilize PSC/PCC tumor foci.

3.2. HDGF in PSCs orchestrates the fibrotic reactions and influences the growth of PCCs

A previous study demonstrated that dense fibrotic reactions serve as a hypovascular barrier [1]. Therefore, penetration of the endothelial cells of blood vessels is appropriate for assessing tissue density. PSCs and PCCs were coimplanted into mice to determine the essentiality of HDGF in PSC-generated fibrotic reactions *in vivo*. Control *shLacZ* or *shHDGF* RLT-PSCs were individually mixed with EGFP/PANC-1 or EGFP/MIA PaCa-2 cells. Picrosirius red staining was performed to examine the abundance of collagens in tissue sections from xenografted tumors of coimplantation of RLT-PSCs and PCCs. The results showed that the abundance of collagens was reduced in xenografted tumor sections of coimplanted *shHDGF* RLT-PSCs and EGFP/PANC-1 or EGFP/MIA PaCa-2 cells (Fig. 2A–B). These results suggest that HDGF is not only involved in ECM protein synthesis *in vitro* but also in ECM protein deposition *in vivo*. Additionally, compared with the GFP-negative region of xenografted tumors composed of *shLacZ* RLT-PSCs, the mean fluorescence intensity of the COL1A2 and FN1 signals was attenuated in the GFP-negative region of xenografted tumors composed of *shHDGF* RLT-PSCs (Fig. 2C–F). The COL1A2 and FN1 signals were also assessed in whole tissue sections, and the results showed that the expression of both COL1A2 and FN1 was decreased in tissue sections composed of *shHDGF* RLT-PSCs and EGFP/PANC-1 or EGFP/MIA PaCa-2 cells (Fig. 2C–F). These results indicate that the diminished deposition of type I collagen and fibronectin is associated with the disruption of fibrotic reactions when *shHDGF* RLT-PSCs are cocultivated with PCCs. Interestingly, the expression of CD31, an angiogenic marker, was enhanced in the xenografted tumor sections of coimplanted *shHDGF* RLT-PSCs and EGFP/PANC-1 or EGFP/MIA PaCa-2 cells (Fig. 2G–H), suggesting that the essentiality of HDGF is involved in the fibrotic hypovascular barrier and attenuates blood vessel penetration. Additionally, compared to individual xenografted tumors of coimplanted *shLacZ* RLT-PSCs and EGFP-bearing PCCs, coimplantation of *shHDGF* RLT-PSCs and EGFP-bearing PCCs showed larger tumor sizes in the *in vivo* imaging system spectrum (Fig. 2I–J). Interestingly, higher levels of mitotic activity and more apoptotic bodies were observed in the PCCs of coimplanted *shHDGF* RLT-PSCs and EGFP/PCCs *in vivo* (Supplementary Fig. 3). These observations suggest that PCCs have a more rapid mitotic rate and a higher apoptotic index when coimplanted with *shHDGF* RLT-PSCs, resulting in less fibrotic reactions. Collectively, our *in vivo* results imply that *HDGF*-deficient PSCs restrain fibrotic reactions and enhance cancer progression.

3.3. TGF-β1/CEBPD/HIF-1α axis contributes to HDGF transcriptional activation in PSCs

We found that TGF-β1-induced HDGF production is synchronous with its transcriptional activation (Figs. 1C, 3A and 3B). We next

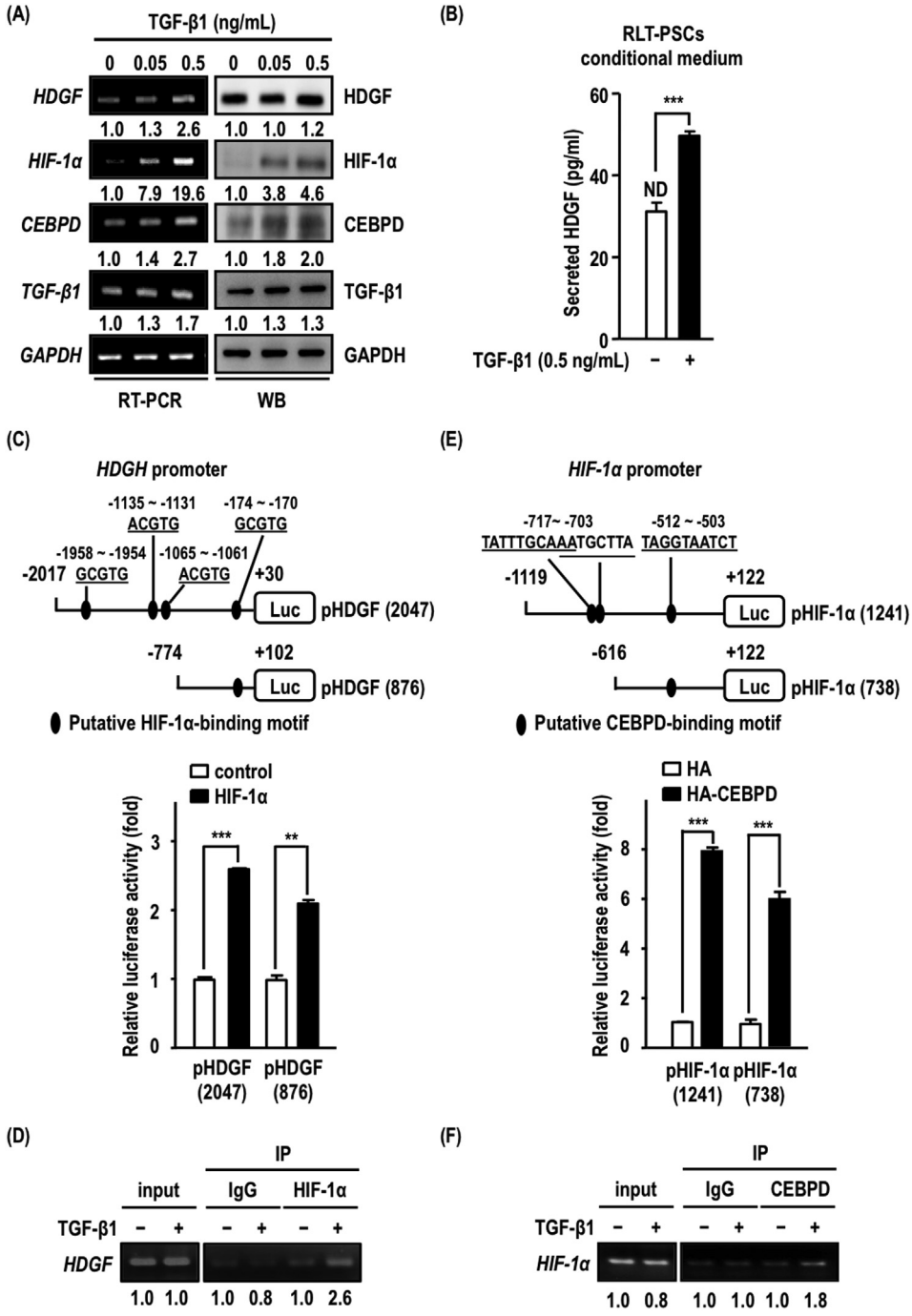

Fig. 3. HDGF is transcriptionally upregulated by the TGF-β1/Hypoxia inducible factor-1α (HIF-1α)/CCAAT/enhancer-binding protein δ (CEBPD) axis.(A) After 0.5 ng/mL of TGF-β1 treatment for 24 h, the mRNA or protein levels of HDGF, HIF-1α, CEBPD, and TGF-β1 were determined using RT-PCR or Western blot assays in RLT-PSCs. (B) After treatment with 0.5 ng/mL TGF-β1 for 24 h, the levels of HDGF in conditioned medium containing 1% bovine serum albumin were determined using an enzyme-linked immunosorbent assay. (ND indicates not detectable; the minimum detectable concentration was 30 pg/mL). (C) The putative HIF-1α-binding motifs on the HDGF promoter region are shown in the upper panel. The HDGF reporter vector was transfected into RLT-PSCs simultaneously with the pCEP4/HIF-1α expressing vector (or the pcDNA3/HA expressing vector as a control group) for 18 h; then, a luciferase reporter assay was performed to confirm the putative HIF-1α-binding motifs on the HDGF promoter region. The results were obtained from three independent experiments and are presented as the mean ± standard error of the mean; the statistical significance was determined using Student's unpaired *t*-test (***P < 0.001). (D) A chromatin immunoprecipitation assay was performed to determine the binding of HIF-1α to the HDGF promoter region in RLT-PSCs treated with 0.5 ng/mL TGF-β1 for 24 h. The IgG antibody was used as a negative control. (E) A luciferase reporter assay was used to confirm the putative CEBPD-binding motifs on the HIF-1α promoter region. The putative CEBPD-binding motifs on the HIF-1α promoter region are shown in the upper panel. RLT-PSCs were transfected with the HIF-1α reporter vector and pcDNA3/HA or pcDNA3/CEBPD expressing vectors for 18 h and subsequently subjected to luciferase reporter assays. The results are presented as the mean ± standard error of the mean, and the statistical significance was determined using Student's unpaired *t*-test (**P < 0.01; ***P < 0.001). (F) The results of the chromatin immunoprecipitation assays showed the interaction between CEBPD and the HIF-1α promoter in RLT-PSCs treated with 0.5 ng/mL TGF-β1 for 24 h. The above data were obtained from three independent experiments.

dissected the transcriptional regulation of determined whether the *HDGF* gene in PSCs. Following the observation of putative HIF-1α-binding motifs on *HDGF* promoter region, we therefore first examined whether HIF-1α was responsive to TGF-β1 in RLT-PSCs. In addition to HDGF expression, both *HIF-1α* mRNA and HIF-1α protein were upregulated in TGF-β1-treated RLT-PSCs (Fig. 3A). HIF-1α is a well-known inducible transcription factor and tends toward stabilization under hypoxic conditions, we tested whether TGF-β1 could stabilize HIF-1α in a normoxic condition. We found that TGF-β1 had no effect on HIF-1α protein stability (Supplementary Fig. 4). Moreover, reporter and ChIP assays showed that HIF-1α was responsive to TGF-β1, activated the *HDGF* reporter and directly bound to the *HDGF* promoter region under normoxic condition (Fig. 3C–D).

Next, we revealed which transcription factor in response to TGF-β1 and contributed to *HIF-1α* transcription in PSCs. Putative CEBPD-binding motifs on the *HIF-1α* promoter were predicted. We further examined whether CEBPD was responsive to TGF-β1 in PSCs. The results showed that TGF-β1 induced *CEBPD* and autoregulated *TGF-β1* transcripts and expression (Fig. 3A). Moreover, the reporter assay showed that the exogenous expression of CEBPD activated the *HIF-1α* reporter in RTL-PSCs (Fig. 3E). Subsequently, a ChIP assay was performed to verify whether CEBPD could bind to the *HIF-1α* promoter upon TGF-β1 stimulation. The results suggested that CEBPD binding was responsive to TGF-β1 and contributed to the *HIF-1α* gene activation in RLT-PSCs (Fig. 3F).

Because the CEBPD/HIF-1α axis contributes to TGF-β1-induced HDGF expression and HDGF contributes to the antiapoptotic activity of PSCs, we further assessed and found both CEBPD and HIF-1α functioned in TGF-β1-induced antiapoptotic activity (Supplementary Figs. 5A–5F).

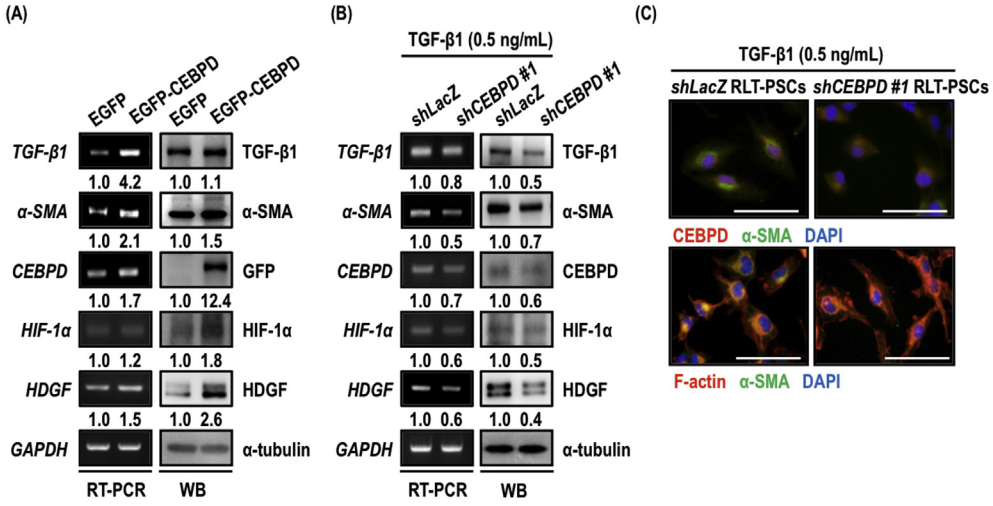

Fig. 4. TGF-β1 induces CEBPD expression through a positive feedback loop.(A) After RLT-PSCs were transfected with pcDNA3/EGFP-CEBPD or the pcDNA/EGFP expressing vector for 18 h, cells were harvested and subjected to RT-PCR and Western blot assays. The mRNA and protein expression levels of α-SMA, CEBPD, HIF-1α, and HDGF were determined in RLT-PSCs with or without CEBPD overexpression. (B) In addition, shLacZ RLT-PSCs and shCEBPD #1 RLT-PSCs were subjected to RT-PCR and Western blot assays to examine the mRNA and protein expression levels of α-SMA, CEBPD, HIF-1α, and HDGF after TGF-β1 treatment (0.5 ng/mL) for 24 h. (C) The fibrogenic markers in TGF-β1-treated RLT-PSCs that could be used to observe morphological changes, such as the high expression of α-SMA and F-actin rearrangement, were determined using immunofluorescence staining in shLacZ RLT-PSCs or shCEBPD #1 RLT-PSCs treated with TGF-β1 (0.5 ng/mL) for 24 h (lower panels). The green and red fluorescence indicate the expression of α-SMA and F-actin, respectively. In addition, CEBPD expression was evaluated in treated cells using immunofluorescence staining (upper panels). The green and red fluorescence indicate the expression of α-SMA and CEBPD, respectively. The white scale bar indicates 100 μm. The above data are representative of three independent experiments. (For interpretation of the references to color in this figure legend, the reader is referred to the Web version of this article.)

3.4. CEBPD responds to TGF-β1 through reciprocal loop regulation

We next assessed the involvement of CEBPD in fibroblast activation via gain- and loss-of-function assays. Following the exogenous expression of CEBPD in RLT-PSCs, the expression of TGF-β1, α-SMA, CEBPD, HIF-1α, and HDGF was induced (Fig. 4A). By contrast, the expression of these proteins was attenuated in *shCEBPD* RLT-PSCs upon TGF-β1 treatment (Fig. 4B; Supplementary Fig. 6A). Interestingly, regarding to CEBPD also upregulated TGF-β1 expression in RLT-PSCs, suggesting a positive feedback regulation between CEBPD and TGF-β1 (Fig. 4A–B). Moreover, TGF-β1-induced F-actin rearrangement was attenuated in *shCEBPD* RLT-PSCs, suggesting the involvement of CEBPD in the fibroblast-to-myofibroblast transition (Fig. 4C; Supplementary Fig. 6B).

3.5. HDGF and CEBPD expression is positively associated with antiapoptosis and severe stromal growth in human pancreatic cancer specimens

The above results suggested that the TGF-β1-activated CEBPD/HIF-1α/HDGF axis in PSCs contributes to antiapoptotic and profibrotic effects that serve as a stabilizer of PSC/PCC tumor foci. We next assessed the clinical relevance of apoptotic activity and COL1A2, HDGF, and CEBPD expression in stromal cells using a commercial tissue array. According to the cell proportion ratio of stromal cells versus total tissue cells, 78 human primary pancreatic cancer specimens were subdivided into mild (< 50%) or severe (≥50%) stromal growth. After examining the expression levels of apoptotic proteins, COL1A2, HDGF, and CEBPD were detected in the stroma in 78 human pancreatic cancer specimens using IF staining. The H-score method, in which two independent expert pathologists assign a score of 0–300 to each specimen, was used to assess the extent of immunoreactivity. Apoptotic activity in the stroma was negatively associated with the levels of stromal HDGF expression (Fig. 5A**, brown color and** Fig. 5B). Stromal COL1A2 expression showed a strong association ($P < 0.001$) with severe stromal growth (Fig. 5A**, red color and 5C**). We also observed a significant association between severe stromal growth and high HDGF or CEBPD expression in the stroma (Fig. 5A**, green and cyan colors**, Fig. 5D–E). These results agree with the above suggestion that HDGF and CEBPD in the stroma contribute to pancreatic cancer-associated fibrosis. According to tumor/node/metastasis (TNM) staging of pathological verification, 78 pancreatic cancer specimens were subdivided into two groups: stage I (group 1) and stages II, III, and IV (group 2). We observed that the H-scores of COL1A2, HDGF, and CEBPD in the stroma showed no significant variation in these two groups (Fig. 5F–H). Stage I pancreatic adenocarcinoma patients with high CEBPD or HDGF expression pursue a more aggressive clinical course and have significantly shorter disease-specific survival (Fig. 5I–J)

Our results suggest that the TGF-β1-activated CEBPD/HIF-1α/HDFG axis in PSCs is involved in antiapoptosis and profibrosis under normoxic conditions *in vitro*. However, most clinical pancreatic cancer tissues are accompanied by strong fibrotic reactions, which are associated with the hypoxic status [6]. Therefore, to specifically assess whether the CEBPD/HIF-1α/HDFG axis promotes fibrosis under hypoxic conditions, a hypoxic marker, carbonic anhydrase IX (CA9) [31], was applied to distinguish the hypoxia/normoxia status of clinical specimens. Following the combination of CA9 abundance and the status of stromal growth, 78 pancreatic cancer specimens were subdivided into four groups: normoxic (low CA9 expression) or hypoxic (high CA9 expression) specimens of pancreatic adenocarcinoma accompanied by mild (< 50%) or severe (≥50%) stromal growth (Fig. 6A–B). The H-score of CA9 was comparable between pancreatic adenocarcinoma specimens with mild and severe stromal growth (Fig. 6C). We found that the higher H-score of stromal CEBPD and HDGF was observed and significantly associated with severe stromal growth in hypoxic specimens of pancreatic adenocarcinoma (Fig. 6D and E**; compared groups 2 and 4**). Importantly, even in normoxic specimens of pancreatic adenocarcinoma, the H-scores of both stromal CEBPD (from 181.4 ± 39.0 to 196.0 ± 29.0) and stromal HDGF (from 211.6 ± 54.6 to 248.5 ± 45.1) were consistently elevated from mild to severe stromal growth (Fig. 6E and F**; compared groups 1 and 3**). However, in normoxic or hypoxic specimens of pancreatic adenocarcinoma that accompanied severe stromal growth, there was no significant difference in the H-score of CEBPD or HDGF in the stroma (Fig. 6E and F**; compared groups 3 and 4**). Collectively, these observations suggest that the TGF-β1-activated CEBPD/HIF-1α/HDFG axis specifically associates with pancreatic cancer-associated fibrosis, but not with normoxia and hypoxia.

4. Discussion

The aim of the present study was to determine HDGF regulation and function in PSCs and its contribution to fibrosis-associated pancreatic

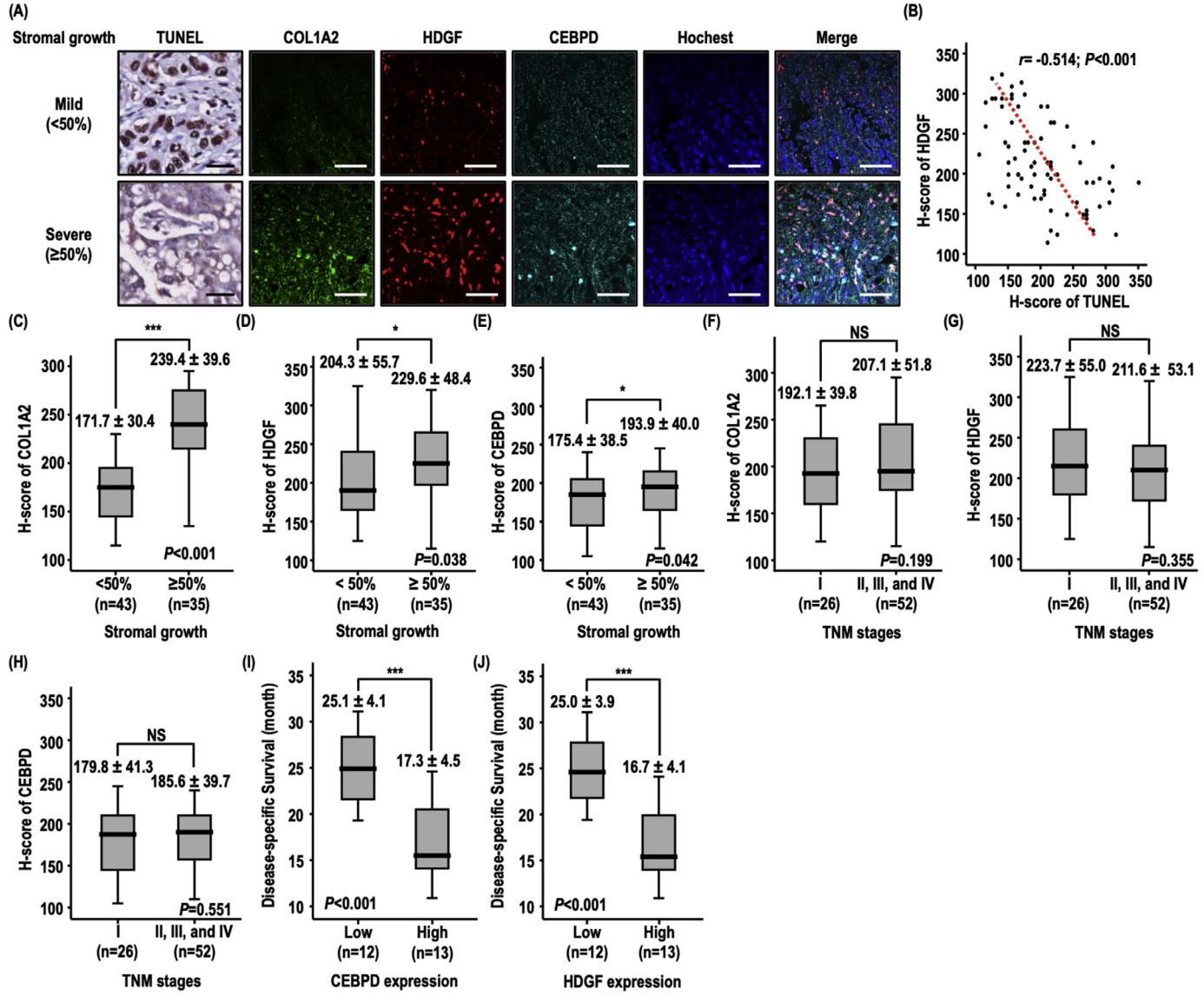

Fig. 5. HDGF and CEBPD are positively associated with antiapoptosis and severe stromal growth in human pancreatic adenocarcinoma specimens. (A) The Opal™ multiplex tissue staining kit was used for immunofluorescence analysis on a commercial tissue array with 78 human primary pancreatic adenocarcinoma specimens. A ratio of cell proportions from stromal cells versus total tissue cells was determined. The 78 human primary pancreatic adenocarcinoma specimens were subdivided into mild (< 50%) or severe (≥ 50%) stromal growth. Apoptotic cells were detected and labeled by brown color using a TUNEL assay kit. Meanwhile, the expression of COL1A2, HDGF, and CEBPD was determined in human pancreatic cancer specimens using immunofluorescence staining and labeled by green, red, and cyan fluorescence, respectively. The black and white scale bars indicate 100 μm. (B) to (E) Histochemistry score (H-score), which assigns a score of 0–300 to each patient by two expert pathologists (CFL and TJC), is applicable to assess the extent of immunoreactivity of TUNEL (B), COL1A2 (C), HDGF (D), and CEBPD (E) in stroma. (B) Pearson's correlation coefficient test was used to observe negative and significant correlations between stromal HDGF and apoptotic activity, which indicated cell apoptosis ($r = -0.541$; $P < 0.001$). (C) to (E) The expression of COL1A2, HDGF, and CEBPD in the stroma was significantly and positively associated with stromal overgrowth. The results are presented as both the mean ± standard error of the mean and median with quartiles. The Mann-Whitney *U* test was used for comparison between two groups, with $P < 0.05$ taken to indicate a significant difference (*$P < 0.05$; **$P < 0.01$; ***$P < 0.001$). (F) to (H) According to tumor/node/metastasis (TNM) staging, 78 pancreatic cancer specimens were grouped into two groups: stage I (group 1) and stages II, III, and IV (group 2). The H-scores of stromal COL1A2, HDGF, and CEBPD were comparable between the two groups. The results are presented as both the mean ± standard error of the mean and median with quartiles. The Mann-Whitney *U* test was used for comparison between two groups, with $P < 0.05$ taken to indicate a significant difference (NS stands for not significant). (I) and (J) The correlation between pancreatic adenocarcinoma patient prognosis and CEBPD or HDGF. The H-score of HDGF (I) and CEBPD (J) was assessed in 25 stage I pancreatic adenocarcinoma specimens treated by the Whipple operation procedure with R0 resection (microscopically margin free). Stage I pancreatic adenocarcinoma patients with high CEBPD or HDGF expression pursue a more aggressive clinical course and have a significantly shorter disease-specific survival rate (both $p < 0.001$). (For interpretation of the references to color in this figure legend, the reader is referred to the Web version of this article.)

cancer. The results demonstrated that TGF-β1 activated HDGF expression through the CEBPD/HIF-1α axis in PSCs. Increased production of HDGF prevented apoptosis and promoted the production of ECM proteins, including COL1A2 and FN1, to stabilize PSC/PCC tumor foci. Importantly, these results suggest that HDGF supports PSCs in orchestrating pancreatic cancer-associated fibrotic reactions and acts as a fibrotic hypovascular barrier to attenuate blood vessel penetration. In contrast, the attenuation of HDGF in PSCs resulted in fewer or looser fibrotic reactions, which could benefit the outgrowth of PCCs (Fig. 7).

Evidence of HDGF autoregulation and contribution to tumorigenesis has been revealed in several types of cancer cells [18,32,33]. In the present study, we revealed that the regulation of HDGF in PSCs

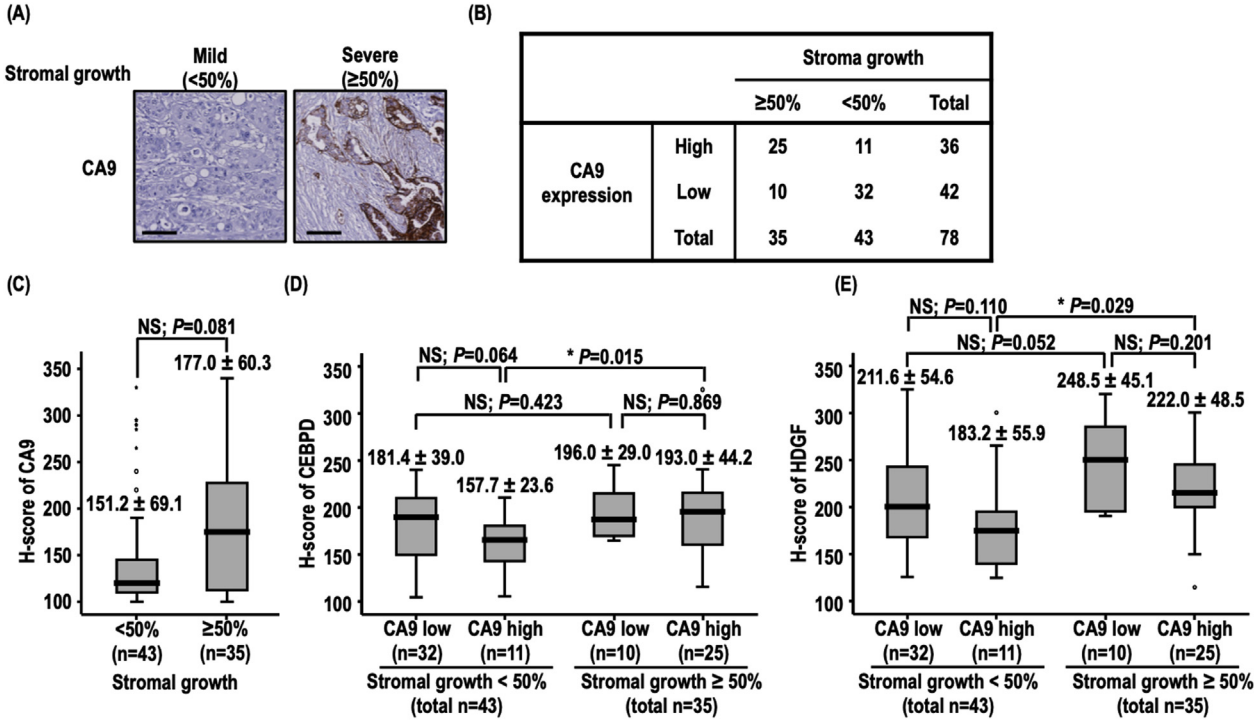

Fig. 6. HDGF and CEBPD are positively associated with antiapoptosis and profibrosis in normoxic and hypoxic human pancreatic adenocarcinoma specimens.(A) An antibody against carbonic anhydrase IX (CA9; as a hypoxic marker) was used for immunohistochemical analysis on a commercial tissue array with 78 human primary pancreatic adenocarcinoma specimens. A ratio of cell proportions from stromal cells versus total tissue cells was determined. The expression of CA9 (brown color) was assigned an H-score by two expert pathologists (CFL and TJC). The black scale bar indicates 200 μm. (B) Furthermore, according to the expression of CA9 and the status of stromal growth, 78 pancreatic cancer specimens were subdivided into four groups: normoxic (CA9 low expression) or hypoxic (CA9 high expression) specimens accompanied by mild (< 50%) or severe (≥ 50%) stromal growth. (C) The expression of CA9 showed comparable levels between mild and severe stromal growth of pancreatic adenocarcinoma specimens. The circle dot indicates the mild outlier, and the asterisk indicates the extreme outlier. (D) and (E) The H-scores of stromal CEBPD and HDGF were selected and compared between two conditions among the four subgroups (normoxic or hypoxic specimens accompanied by mild or severe stromal growth). The above results are presented as both the mean ± standard error of the mean and median with quartiles. The Mann-Whitney *U* test was used for comparison between two groups, with P < 0.05 taken to indicate a significant difference (NS stands for not significant; circle dot indicates the mild outlier of H-score in the 78 human primary pancreatic adenocarcinoma specimens). (For interpretation of the references to color in this figure legend, the reader is referred to the Web version of this article.)

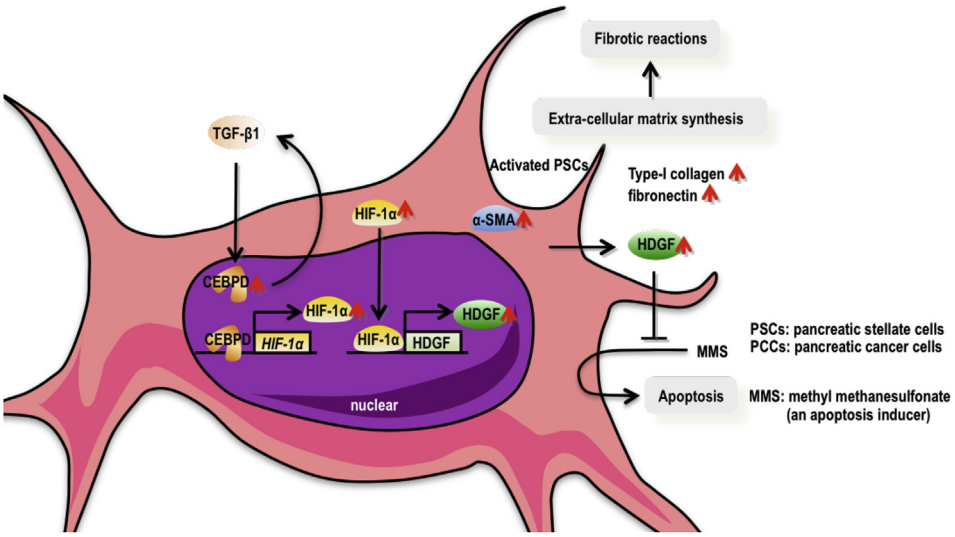

Fig. 7. A schematic illustration of a signaling pathway in pancreatic stellate cells to construct fibrotic reactions. TGF-β1-treated PSCs secreted HDGF through the TGF-β1/CEBPD/HIF-1α axis. The effects of HDGF on PSCs were antiapoptotic under methyl methanesulfonate stimulation. Additionally, HDGF acted as a profibrotic factor, since its expression was required for TGF-β1-treated PSCs to synthesize and deposit extracellular matrix proteins, such as type I collagen and fibronectin. These results suggest roles for HDGF in antiapoptosis and profibrosis in PSCs. Furthermore, TGF-β1 was induced by CEBPD through reciprocal regulation. These results suggest that CEBPD serves as an upstream mediator to regulate HDGF expression in PSCs. Collectively, HDGF or CEBPD could be a therapeutic target to nullify pancreatic cancer-associated fibrosis.

contributed to antiapoptosis, formation of fibrotic hypovascular barrier and attenuated penetration of blood vessel. Moreover, an *in vivo* animal study demonstrated that *HDGF*-deficient PSCs restrain fibrotic reactions and enhance cancer progression. These results in part agree with the observation that physical restraint is partially regained under less fibrotic reactions and that blood moves to tumors through penetrating blood vessels [8]. Clinically, malignant cancers associate with more apoptosis [34]. Our results are shown in Fig. 2I and J **and** Supplementary Fig. 3, suggesting stroma is a non-negligible part in pancreatic cancer progression and stromal HDGF could paly a functional role in the phenomenon.

Remarkably, fibrosis occurred in each TNM stage of pancreatic

cancer; no positive correlation was observed between stromal HDGF or CEBPD expression and malignancies of pancreatic cancers at various TNM stages, suggesting that the fibrotic involvement of HDGF or CEBPD in the development of pancreatic cancer starts from an early stage with normoxia. A previous study suggested that precise quantitation of fibrosis levels in pancreatic cancer should be combined to determine the stage of the disease, to select optimal therapies, and to monitor or predict patient therapeutic outcomes [35]. The present study suggests that HDGF and CEBPD contribute to the interplay of PSCs and PCCs via the deposition of ECM proteins and can serve as a biomarker to evaluate the fibrotic status of pancreatic cancer.

Targeting tumors is currently a major tumor therapeutic strategy. Accumulating studies have highlighted the importance of the tumor microenvironment in benefiting cancer progression [36]. The results of the present study demonstrate that HDGF is involved in the anti-apoptosis of PSCs in pancreatic cancer-associated fibrosis via the CEBPD/HIF-1α axis. However, two previous studies demonstrated that the depletion of α-SMA-positive fibroblasts [7] or the loss of sonic hedgehog protein [8] reduces fibrotic reactions and accelerates tumor progression, including enhanced tumor growth and angiogenesis, in undifferentiated and invasive tumors, with reduced animal survival. Therefore, in the future, the application of therapeutic strategies targeting CEBPD or HDGF in PSCs for reducing fibrotic reactions should be combined with therapeutic drugs to kill pancreatic cancer cells or prevent their metastasis and invasion.

Declarations

Competing interests

No potential conflicts of interest were to disclose.

Funding

This work was financially supported by the National Science Council Taiwan Grants (NHRI-EX106-10422BI from the National Health Research Institute and MOST 106-2320-B-006-063-MY3 from the Ministry of Science and Technology) and Chi Mei Medical Center Research Taiwan Grant #10501.

Authors' contributions

Y.-T. Chen contributed to experiment design, experiment performance, data analysis and result interpretation and manuscript writing. F.-W. Chen performed the quantitative PCR assay and migration assay for the revised manuscript. T.-H. Chang assisted animal studies and provided writing suggestion. T.-W. Wang performed luciferase reporter assay and part of immunofluorescence staining. T.-P. Hsu performed chromatin immunoprecipitation assay and lenti-virus production. J.-Y. Chi and Y.-W. Hsiao generated *mCherry* fluorescent expression vector. C.-F. Li assisted clinical studies, designed experiments and edited manuscript. J.-M. Wang directed the project and edited manuscript.

Ethics approval and consent to participate

The animal experiments were approved by the Institutional Animal Care and Use Committee of National Cheng Kung University (IACUC number 03239). Experiments performed on human samples were approved by the institutional review board of Chi Mei Medical Center (10606-E03).

Acknowledgments

We are grateful for the experimental material providing from Dr. Kelvin K.-C. Tsai (National Health Research Institutes, Taiwan), Dr. Yan-Shen Shan (National Cheng Kung University Hospital, Taiwan), Professor Shaw-Jenq Tsai (National Cheng Kung University, Taiwan), and Professor Ming-Hong Tai (National Sun Yat-sen University, Taiwan). Dr. Tzu-Ju Chen (Chi Mei Medical Center, Taiwan) assisted the pathological re-evaluation of immunohistochemistry analysis.

Appendix A. Supplementary data

Supplementary data to this article can be found online at https://doi.org/10.1016/j.canlet.2019.05.001.

References

[1] K.P. Olive, M.A. Jacobetz, C.J. Davidson, A. Gopinathan, D. McIntyre, D. Honess, B. Madhu, M.A. Goldgraben, M.E. Caldwell, D. Allard, K.K. Frese, G. Denicola, C. Feig, C. Combs, S.P. Winter, H. Ireland-Zecchini, S. Reichelt, W.J. Howat, A. Chang, M. Dhara, L. Wang, F. Ruckert, R. Grutzmann, C. Pilarsky, K. Izeradjene, S.R. Hingorani, P. Huang, S.E. Davies, W. Plunkett, M. Egorin, R.H. Hruban, N. Whitebread, K. McGovern, J. Adams, C. Iacobuzio-Donahue, J. Griffiths, D.A. Tuveson, Inhibition of Hedgehog signaling enhances delivery of chemotherapy in a mouse model of pancreatic cancer, Science 324 (2009) 1457–1461.

[2] H. Habisch, S. Zhou, M. Siech, M.G. Bachem, Interaction of stellate cells with pancreatic carcinoma cells, Cancers 2 (2010) 1661–1682.

[3] M.V. Apte, R.C. Pirola, J.S. Wilson, Pancreatic stellate cells: a starring role in normal and diseased pancreas, Front. Physiol. 3 (2012) 344.

[4] Y. Fu, S. Liu, S. Zeng, H. Shen, The critical roles of activated stellate cells-mediated paracrine signaling, metabolism and onco-immunology in pancreatic ductal adenocarcinoma, Mol. Cancer 17 (2018) 62.

[5] A. Masamune, K. Kikuta, T. Watanabe, K. Satoh, M. Hirota, T. Shimosegawa, Hypoxia stimulates pancreatic stellate cells to induce fibrosis and angiogenesis in pancreatic cancer, Am. J. Physiol. Gastrointest. Liver Physiol. 295 (2008) G709–G717.

[6] M. Erkan, C. Reiser-Erkan, C.W. Michalski, S. Deucker, D. Sauliunaite, S. Streit, I. Esposito, H. Friess, J. Kleeff, Cancer-stellate cell interactions perpetuate the hypoxia-fibrosis cycle in pancreatic ductal adenocarcinoma, Neoplasia 11 (2009) 497–508.

[7] B.C. Ozdemir, T. Pentcheva-Hoang, J.L. Carstens, X. Zheng, C.C. Wu, T.R. Simpson, H. Laklai, H. Sugimoto, C. Kahlert, S.V. Novitskiy, A. De Jesus-Acosta, P. Sharma, P. Heidari, U. Mahmood, L. Chin, H.L. Moses, V.M. Weaver, A. Maitra, J.P. Allison, V.S. LeBleu, R. Kalluri, Depletion of carcinoma-associated fibroblasts and fibrosis induces immunosuppression and accelerates pancreas cancer with reduced survival, Cancer Cell 25 (2014) 719–734.

[8] A.D. Rhim, P.E. Oberstein, D.H. Thomas, E.T. Mirek, C.F. Palermo, S.A. Sastra, E.N. Dekleva, T. Saunders, C.P. Becerra, I.W. Tattersall, C.B. Westphalen, J. Kitajewski, M.G. Fernandez-Barrena, M.E. Fernandez-Zapico, C. Iacobuzio-Donahue, K.P. Olive, B.Z. Stanger, Stromal elements act to restrain, rather than support, pancreatic ductal adenocarcinoma, Cancer Cell 25 (2014) 735–747.

[9] J. Kota, J. Hancock, J. Kwon, M. Korc, Pancreatic cancer: stroma and its current and emerging targeted therapies, Cancer Lett. 391 (2017) 38–49.

[10] A.J. Majmundar, W.J. Wong, M.C. Simon, Hypoxia-inducible factors and the response to hypoxic stress, Mol. Cell 40 (2010) 294–309.

[11] C.Y. Ko, W.C. Chang, J.M. Wang, Biological roles of CCAAT/Enhancer-binding protein delta during inflammation, J. Biomed. Sci. 22 (2015) 6.

[12] C.F. Li, H.H. Tsai, C.Y. Ko, Y.C. Pan, C.J. Yen, H.Y. Lai, C.H. Yuh, W.C. Wu, J.M. Wang, HMDB and 5-AzadC combination reverses tumor suppressor CCAAT/Enhancer-Binding protein delta to strengthen the death of liver cancer cells, Mol. Cancer Ther. 14 (2015) 2623–2633.

[13] J.Y. Chi, Y.W. Hsiao, C.F. Li, Y.C. Lo, Z.Y. Lin, J.Y. Hong, Y.M. Liu, X. Han, S.M. Wang, B.K. Chen, K.K. Tsai, J.M. Wang, Targeting chemotherapy-induced PTX3 in tumor stroma to prevent the progression of drug-resistant cancers, Oncotarget 6 (2015) 23987–24001.

[14] Y.W. Hsiao, C.F. Li, J.Y. Chi, J.T. Tseng, Y. Chang, L.J. Hsu, C.H. Lee, T.H. Chang, S.M. Wang, D.D. Wang, H.C. Cheng, J.M. Wang, CCAAT/enhancer binding protein delta in macrophages contributes to immunosuppression and inhibits phagocytosis in nasopharyngeal carcinoma, Sci. Signal. 6 (2013) ra59.

[15] C. Jiang, J. Sun, Y. Dai, P. Cao, L. Zhang, S. Peng, Y. Zhou, G. Li, J. Tang, J. Xiang, HIF-1A and C/EBPs transcriptionally regulate adipogenic differentiation of bone marrow-derived MSCs in hypoxia, Stem Cell Res. Ther. 6 (2015) 21.

[16] J. Yamaguchi, T. Tanaka, N. Eto, M. Nangaku, Inflammation and hypoxia linked to renal injury by CCAAT/enhancer-binding protein delta, Kidney Int. 88 (2015) 262–275.

[17] H. Enomoto, H. Nakamura, W. Liu, S. Nishiguchi, Hepatoma-derived growth factor: its possible involvement in the progression of hepatocellular carcinoma, Int. J. Mol. Sci. 16 (2015) 14086–14097.

[18] Y. Kishima, H. Yamamoto, Y. Izumoto, K. Yoshida, H. Enomoto, M. Yamamoto, T. Kuroda, H. Ito, K. Yoshizaki, H. Nakamura, Hepatoma-derived growth factor stimulates cell growth after translocation to the nucleus by nuclear localization signals, J. Biol. Chem. 277 (2002) 10315–10322.

[19] S. Yamamoto, Y. Tomita, Y. Hoshida, S. Takiguchi, Y. Fujiwara, T. Yasuda, Y. Doki, K. Yoshida, K. Aozasa, H. Nakamura, M. Monden, Expression of hepatoma-derived growth factor is correlated with lymph node metastasis and prognosis of gastric carcinoma, Clin. Cancer Res. 12 (2006) 117–122.

[20] S.C. Chen, M.L. Kung, T.H. Hu, H.Y. Chen, J.C. Wu, H.M. Kuo, H.E. Tsai, Y.W. Lin,

Z.H. Wen, J.K. Liu, M.H. Yeh, M.H. Tai, Hepatoma-derived growth factor regulates breast cancer cell invasion by modulating epithelial–mesenchymal transition, J. Pathol. 228 (2012) 158–169.
[21] T.C. Shih, Y.J. Tien, C.J. Wen, T.S. Yeh, M.C. Yu, C.H. Huang, Y.S. Lee, T.C. Yen, S.Y. Hsieh, MicroRNA-214 downregulation contributes to tumor angiogenesis by inducing secretion of the hepatoma-derived growth factor in human hepatoma, J. Hepatol. 57 (2012) 584–591.
[22] A.Y. Wehr, E.E. Furth, V. Sangar, I.A. Blair, K.H. Yu, Analysis of the human pancreatic stellate cell secreted proteome, Pancreas 40 (2011) 557–566.
[23] W.Y. Wang, C.C. Hsu, T.Y. Wang, C.R. Li, Y.C. Hou, J.M. Chu, C.T. Lee, M.S. Liu, J.J. Su, K.Y. Jian, S.S. Huang, S.S. Jiang, Y.S. Shan, P.W. Lin, Y.Y. Shen, M.T. Lee, T.S. Chan, C.C. Chang, C.H. Chen, I.S. Chang, Y.L. Lee, L.T. Chen, K.K. Tsai, A gene expression signature of epithelial tubulogenesis and a role for ASPM in pancreatic tumor progression, Gastroenterology 145 (2013) 1110–1120.
[24] M.C. Yang, H.C. Wang, Y.C. Hou, H.L. Tung, T.J. Chiu, Y.S. Shan, Blockade of autophagy reduces pancreatic cancer stem cell activity and potentiates the tumoricidal effect of gemcitabine, Mol. Cancer 14 (2015) 179.
[25] P.H. Lai, W.L. Wang, C.Y. Ko, Y.C. Lee, W.M. Yang, T.W. Shen, W.C. Chang, J.M. Wang, HDAC1/HDAC3 modulates PPARG2 transcription through the sumoylated CEBPD in hepatic lipogenesis, Biochim. Biophys. Acta 1783 (2008) 1803–1814.
[26] Y. Sakurai, T. Sawada, Y.S. Chung, Y. Funae, M. Sowa, Identification and characterization of motility stimulating factor secreted from pancreatic cancer cells: role in tumor invasion and metastasis, Clin. Exp. Metastasis 15 (1997) 307–317.
[27] M.A. Shields, S. Dangi-Garimella, A.J. Redig, H.G. Munshi, Biochemical role of the collagen-rich tumour microenvironment in pancreatic cancer progression, Biochem. J. 441 (2012) 541–552.
[28] R. Jesnowski, D. Furst, J. Ringel, Y. Chen, A. Schrodel, J. Kleeff, A. Kolb, W.D. Schareck, M. Lohr, Immortalization of pancreatic stellate cells as an in vitro model of pancreatic fibrosis: deactivation is induced by matrigel and *N*-acetylcysteine, Lab. Investig. 85 (2005) 1276–1291.
[29] B.N. Ooi, A. Mukhopadhyay, J. Masilamani, D.V. Do, C.P. Lim, X.M. Cao, I.J. Lim, L. Mao, H.N. Ren, H. Nakamura, T.T. Phan, Hepatoma-derived growth factor and its role in keloid pathogenesis, J. Cell Mol. Med. 14 (2010) 1328–1337.
[30] A. Suetsugu, C.S. Snyder, H. Moriwaki, S. Saji, M. Bouvet, R.M. Hoffman, Imaging the interaction of pancreatic cancer and stellate cells in the tumor microenvironment during metastasis, Anticancer Res. 35 (2015) 2545–2551.
[31] M. Barathova, M. Takacova, T. Holotnakova, A. Gibadulinova, A. Ohradanova, M. Zatovicova, A. Hulikova, J. Kopacek, S. Parkkila, C.T. Supuran, S. Pastorekova, J. Pastorek, Alternative splicing variant of the hypoxia marker carbonic anhydrase IX expressed independently of hypoxia and tumour phenotype, Br. J. Canc. 98 (2008) 129–136.
[32] R. Song, L. Cong, G. Ni, M. Chen, H. Sun, Y. Sun, M. Chen, MicroRNA-195 inhibits the behavior of cervical cancer tumors by directly targeting HDGF, Oncol Lett 14 (2017) 767–775.
[33] Y. Yang, H. Li, F. Zhang, H. Shi, T. Zhen, S. Dai, L. Kang, Y. Liang, J. Wang, A. Han, Clinical and biological significance of hepatoma-derived growth factor in Ewing's sarcoma, J. Pathol. 231 (2013) 323–334.
[34] R.A. Wang, Q.L. Li, Z.S. Li, P.J. Zheng, H.Z. Zhang, X.F. Huang, S.M. Chi, A.G. Yang, R. Cui, Apoptosis drives cancer cells proliferate and metastasize, J. Cell Mol. Med. 17 (2013) 205–211.
[35] W. Li, Z. Zhang, J. Nicolai, G.Y. Yang, R.A. Omary, A.C. Larson, Quantitative magnetization transfer MRI of desmoplasia in pancreatic ductal adenocarcinoma xenografts, NBM (NMR Biomed.) 26 (2013) 1688–1695.
[36] A. Neesse, H. Algul, D.A. Tuveson, T.M. Gress, Stromal biology and therapy in pancreatic cancer: a changing paradigm, Gut 64 (2015) 1476–1484.